

REPORT DOCUMENTATION PAGE

Form Approved
OMB No. 0704-0188

Public reporting burden for this collection of information is estimated to average 1 hour per response, including the time for reviewing instructions, searching data sources, gathering and maintaining the data needed, and completing and reviewing the collection of information. Send comments regarding this burden estimate or any other aspect of this collection of information, including suggestions for reducing this burden to Washington Headquarters Service, Directorate for Information Operations and Reports, 1215 Jefferson Davis Highway, Suite 1204, Arlington, VA 22202-4302, and to the Office of Management and Budget, Paperwork Reduction Project (0704-0188) Washington, DC 20503.

PLEASE DO NOT RETURN YOUR FORM TO THE ABOVE ADDRESS.

1. REPORT DATE (DD-MM-YYYY) 06-12-2013		2. REPORT TYPE Final Report		3. DATES COVERED (From - To) 3/30/2012 - 3/29/2013	
4. TITLE AND SUBTITLE Fundamental Understanding of the Impact High Pulsed Power Loading has on a MicroGrid's DC or AC Bus				5a. CONTRACT NUMBER	
				5b. GRANT NUMBER N00014-12-1-0594	
				5c. PROGRAM ELEMENT NUMBER	
6. AUTHOR(S) David A. Wetz Jr.				5d. PROJECT NUMBER	
				5e. TASK NUMBER	
				5f. WORK UNIT NUMBER	
7. PERFORMING ORGANIZATION NAME(S) AND ADDRESS(ES) University of Texas at Arlington 701 S. Nedderman, Box 19145 Arlington, Texas, 76019-0145				8. PERFORMING ORGANIZATION REPORT NUMBER	
9. SPONSORING/MONITORING AGENCY NAME(S) AND ADDRESS(ES) Office of Naval Research, 140 Sylvester Road Bldg. 140, Room 21B San Diego, California, 92106-3521				10. SPONSOR/MONITOR'S ACRONYM(S) ONR	
				11. SPONSORING/MONITORING AGENCY REPORT NUMBER	
12. DISTRIBUTION AVAILABILITY STATEMENT Approved for Public Release - Distribution Unlimited					
13. SUPPLEMENTARY NOTES					
14. ABSTRACT Seamless integration of distributed/renewable energy into a smart MicroGrid architecture is a hot topic of research for both public and defense applications. It is the DoD's intention to develop a more cost efficient and reliable power architecture on the battlefield. A smart MicroGrid seamlessly integrates an array of locally installed, distributed power sources and couples them using advanced control schemes to improve the reliability at the sources' point of common coupling. These islanded grids must be capable of powering a wide range of conventional and advanced loads including climate control systems, lights, communication systems, and high pulsed power systems such as radars, high power microwave (HPM) weapons, or electromagnetic launchers among others. The latter types of loads draw rapid high power bursts of energy from the grid and are typically powered using their own dedicated power supplies. The impact this type of loading has on the central DC or AC bus of a MicroGrid must be studied and it was the intent of this research to better understand how operation of these advanced loads impacts the quality of the voltage on the main bus of a MicroGrid.					
15. SUBJECT TERMS Energy Storage, MicroGrid, Pulsed Power, Power Density, Hybrid Energy Storage, Distributed Electrical Generation					
16. SECURITY CLASSIFICATION OF:			17. LIMITATION OF ABSTRACT UU	18. NUMBER OF PAGES 19	19a. NAME OF RESPONSIBLE PERSON David A. Wetz Jr., Ph.D.
a. REPORT U	b. ABSTRACT U	c. THIS PAGE U			19b. TELEPHONE NUMBER (Include area code) (817)272-1058

Final Report
Fundamental Understanding of the Impact
High Pulsed Power Loading has on a
MicroGrid's DC or AC Bus

Submitted to:

Mr. Donald Hoffman
donald.hoffman@navy.mil
and
Mr. John Heinzl
john.heinzl@navy.mil

Grant Number N00014-12-1-0594

Performance Period: March 30, 2012 – March 29, 2013

Submitted by:

David Alan Wetz Jr., Ph.D
Assistant Professor
University of Texas at Arlington
College of Engineering
Electrical Engineering Department
416 Yates Street
537 Nedderman Hall
Arlington, Texas 76019-0016
Phone: (817) 272-1058

20130627049

Abstract

Seamless integration of distributed/renewable energy into a smart MicroGrid architecture is a hot topic of research for both public and defense applications. It is the DoD's intention to develop a more cost efficient and reliable power architecture on the battlefield. A smart MicroGrid seamlessly integrates an array of locally installed, distributed power sources and couples them using advanced control schemes to improve the reliability at the sources' point of common coupling. These islanded grids must be capable of powering a wide range of conventional and advanced loads including climate control systems, lights, communication systems, and high pulsed power systems such as radars, high power microwave (HPM) weapons, or electromagnetic launchers among others. The latter types of loads draw rapid high power bursts of energy from the grid and are typically powered using their own dedicated power supplies. The impact this type of loading has on the central DC or AC bus of a MicroGrid must be studied and it was the intent of this research to better understand how operation of these advanced loads impacts the quality of the voltage on the main bus of a MicroGrid.

Introduction

The intent of the research documented here was to investigate how the power quality is impacted when high power and low impedance loads are sourced on a MicroGrid platform [1-4]. Furthermore, the work was aimed at understanding how the stiffness and impedance of different distributed generation sources, including electrochemical energy storage devices. Most conventional electrical grids primarily rely on the conversion of the chemical energy in fossil fuels to electrical energy. Fossil fuels are dirty, expensive, and make us reliable upon many foreign nations from which they originate. In order to become a more reliable and efficient fleet, the Navy has visions of becoming a more electric fleet. This involves the introduction of additional forms of distributed electrical generation, including wind turbines, solar panels, fuel cells, rechargeable batteries, capacitors, flywheels, etc with those installed varying upon the type and needs of the platform on which they are being installed. The stiffness, reliability, power density, and energy density of these sources varies significantly and therefore must be carefully characterized and evaluated prior to use in a Navy application. The uncertainty of use for the Navy is further escalated by the need to drive extremely high pulsed and continuous power loads including radar stations, communications stations, directed energy weapon systems, and electric propulsion systems among others in addition to the conventional loads most are already familiar with. These high power loads will source energy from the various distributed power sources simultaneously and for that reason it becomes necessary to understand how the different sources will interact, how the different properties described above influence where the power comes from, and how the quality of the power delivered to the source is affected. In order to meet the needs of these high power loads, it has been proposed that a hybrid energy storage module, which combines devices with both high power and high energy densities [4-5].

With support from the US DoE under grant number DE-OE000036 from April 2010 – April 2013, we installed a digitally controllable MicroGrid testbed at UTA that enables us to better understand how distributed generation sources (DESS) can power various high power loads discussed earlier in a reliable fashion. The installed DESS include 4 – 300 W vertical axis wind turbines (VAWT), 12 – 230 W solar panels, a 6 kW diesel generator, 1 – 1.2 kW proton exchange membrane (PEM) fuel cell, 24 V DC bus enabling various forms of energy storage installation, and finally a connection to the legacy electrical grid. All of these DESS are currently configured into three independent MicroGrids which can operate independent of one another or in an interconnected fashion. A simple graphical schematic diagram of the current MicroGrid testbed is shown in Figure 1.

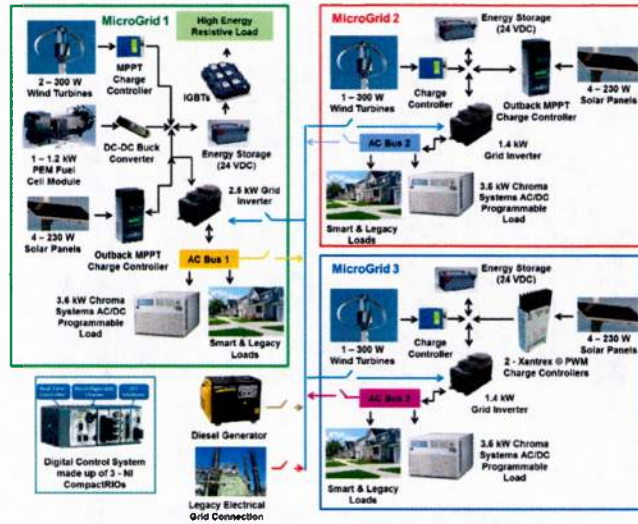


Figure 1. Simple schematic diagram of the UTA MicroGrid testbed.

Utilizing the support from the ONR Grant documented here, the grid was reconfigured to drive DC loads directly from the energy storage in addition to 120V - 60 Hz AC loads via the inverters. This was done as a means to understand how the integration of high power and transient DC loads impacts the MicroGrid's DC and AC voltage buses, especially when low inertia DESs are installed [6]. Examples of low inertia DESs are wind and solar energy conversion systems since they are subject to fast fluctuation. Due to this fluctuation, they may not be able to source the power required for high transient loads such as inrush currents on motors or pulsed charging of capacitors. The stiffer DESs installed on the MicroGrid, such as a diesel generator or the local utility grid should support these types of loads, but they may not always be available either due to system outages or the high cost associated with drawing power from them. Fuel cells provide a stable renewable option; however, fuel cells typically have more energy density than power density. Installation of power dense energy storage technologies may serve as the more stable solution for sourcing high current transient loads.

In order to draw high power loads from the DC bus, two Insulated-Gate-Bipolar-Junction (IGBT) transistors were connected in parallel between the energy storage and a high power adjustable impedance load was installed as well. Each switch can hold off 1.7 kV, conduct 2.4 kA continuously as long as the collector temperature stays below 80°C, and can conduct a peak surge current of 20 kA for roughly 10 ms. In the experiments presented here, a low impedance load that is almost purely resistive is used. A series/parallel connection of up to 20 – 100 mΩ high energy disk resistors enable the load to vary easily from roughly 8 mΩ up to 2 Ohms. Photographs of various portions of the MicroGrid testbed are shown in Figures 2 – 4. Using the grid, a number of experiments were performed utilizing the funding from this ONR Grant. A few of those which provided the most interesting results will be discussed next.

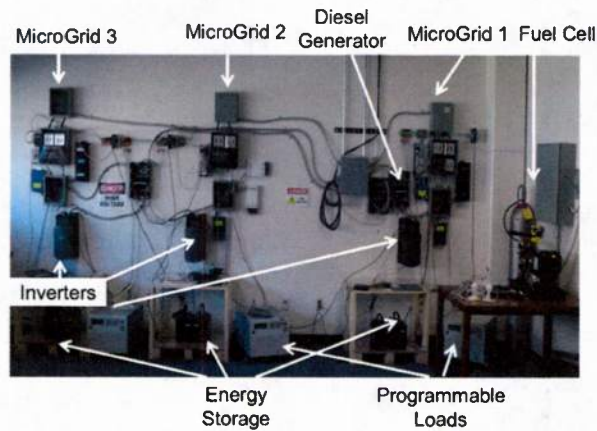


Figure 2. Laboratory photograph of the MicroGrid testbed.



Figure 3. Photograph of the solar, wind, and diesel generator DESs on the laboratory roof.

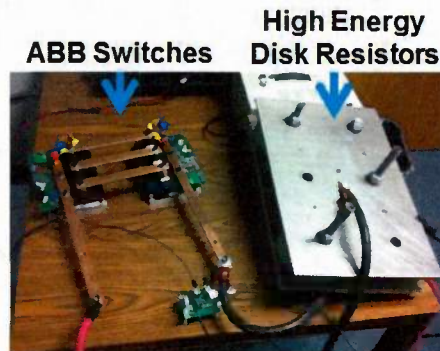


Figure 4. Photograph of the IGBT switches and the high power resistive load in the 50 mΩ configuration. (High energy disk resistors are sandwiched between two aluminum plates)

Experimental Results

Commissioning Results

In the final experiments presented, two different types of electrochemical energy storage were connected on MicroGrid 1, one lithium-ion module and one lead-acid module. Each module was pulse loaded for 15 ms into a 50 mΩ high energy load. Two experiments will be shown. The only difference between them was the type of module that connected on the grid. MicroGrids 2 and 3 were not used. Over

the time period when testing was conducted, the weather remained perfectly calm on every day testing was conducted, removing any contribution from the wind turbines. On the flip side, it was very warm and sunny making solar energy plentiful. Therefore the fuel cell and the solar panels supplied energy to the inverter, pulsed load, and energy storage modules. None of the batteries were fully charged during testing which allowed them to accept current from the renewable sources prior to the system being pulsed loaded.

The aim of the experiments presented was to commission the experimental setup. The lithium-ion battery module is made up of two parallel stacks of six 4.1 V GAIA 27 Ah cells providing a 54 Ah, 24.4 V source voltage with a $\sim 3.0 \text{ m}\Omega$ ESR [7]. The lead-acid battery module is made up of a series connection of two DieHard® marine, 100 Ah, 1150 cold cranking amp batteries [8]. The lead acid module voltage hovered around roughly 26.5 V and had an ESR of $\sim 6.3 \text{ m}\Omega$. Photographs of the two modules are shown in Figure 5.



Figure 5. 100 Ah Gel cell lead-acid (left) and 54 Ah GAIA lithium-ion battery (right) energy storage modules.

During each experiment, the output of the buck converter, which is connected between the fuel cell and the energy storage, was set to 26.4 V. The impact a high current pulsed discharge has on the operation of the fuel cell is a big question since it is the stiffest, low power density source in the system. A 100 W light bulb was connected across the output of the 120 VAC, 60 Hz inverter. The results obtained from the two experiments are presented in Figure 6 through Figure 12.

First, a plot of each battery module’s current and voltage are shown in Figure 6. Due to the lithium-ion batteries lower ESR, the voltage decrease during the high current pulse is roughly half that of the lead acid module. This higher conduction voltage will help to maintain the DC bus quality, especially when the pulsed currents are increased further.

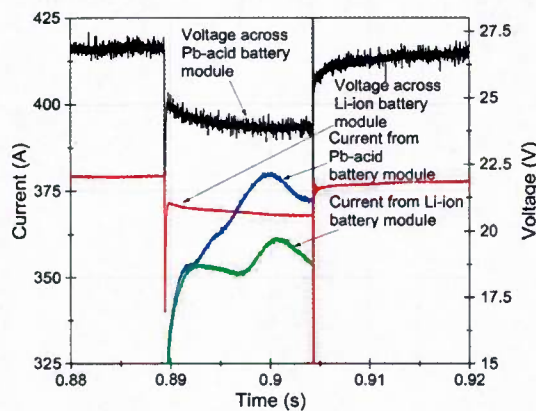


Figure 6. Energy storage module voltage and current.

In Figure 7, the current supplied by the solar panels and the fuel cell is plotted when each of the two energy storage modules were used. The current output from each of their respective charge controllers is plotted in Figure 8 and the solar panel and fuel cell output voltages are plotted in Figure 9.

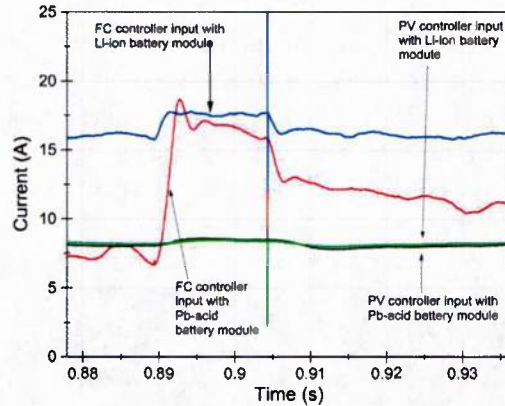


Figure 7. Current sourced by the fuel cell and solar energy modules into their respective charge controllers. (zero current was supplied from the wind turbines as the cut-in wind speed was never reached during the time of testing)

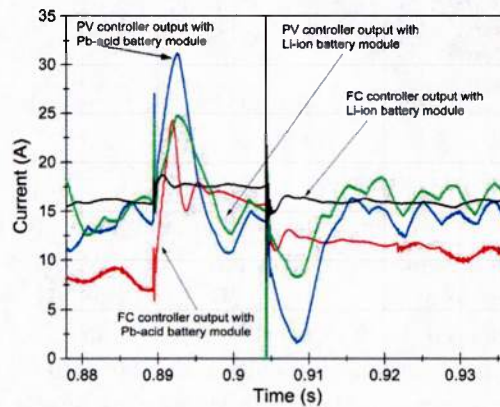


Figure 8. Current sourced by the fuel cell and solar energy charge controllers into the energy storage modules, inverter, and pulsed load. (zero current was supplied from the wind turbines as the cut-in wind speed was never reached during the time of testing)

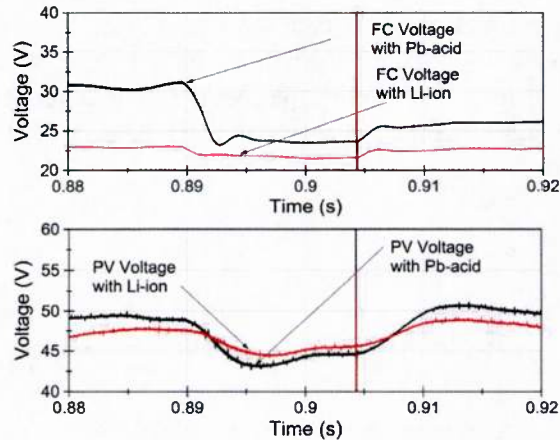


Figure 9. Fuel cell and solar panel output voltage.

The 15 ms pulsed discharge began just shy of 0.89 s. Because the lithium-ion module had a lower voltage relative to Buck converter, the steady state current sourced to it was higher than it was to the lead-acid battery. During the 15 ms pulsed discharge, there is a noticeable impact to the current output of both the fuel cell and the solar panels. The change in the current supplied to the load by the fuel cell's Buck converter and the fuel cell itself as a result, is higher when the lead acid batteries were used as opposed to the lithium-ion module. The likely cause for this is the difference in the ESR's of the two modules. The buffer capacitance on the output of the buck converter is likely lower than that of the lead-acid module and therefore it contributes more to the load. In the case of the lithium-ion batteries, the ESR of the module and the buffer capacitance are more comparable causing the batteries to contribute more to the initial current rise in that case. Similarly, there is a noticeable rise in the current sourced by the solar panels and its controller; though the rise is not as significant compared to the fuel cell. The contribution from the controller is slightly higher when the lead acid batteries were used as opposed to the lithium-ion cells. The current drawn by the DC to AC inverter is shown in Figure 10. As the 15 ms pulse begins, current is actually sourced from the inverter's DC bus capacitance. Roughly 50 A is sourced when the lead acid batteries are used as opposed to nearly 30 A when the lithium-ion batteries are used. Because the lithium-ion battery ESR is lower than that of the lead-acid, it contributes more to the rise time of the discharge relying less on the low ESR of the inverter's bus capacitance. At the conclusion of the pulse, the inverter reabsorbs similar currents to restore the DC bus voltage to its nominal value.

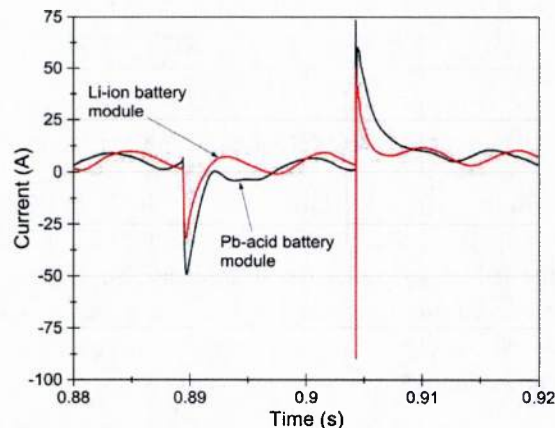


Figure 10. Current drawn and sourced by the inverter during the two experiments.

The current drawn by the 50 mΩ resistive load and that sourced by each energy storage module is shown in Figure 11. The full ~400 A pulse is shown in the upper portion of the plot and a zoomed in view of the peaks is shown in the lower portion. While the energy storage sources most of the current in either case, the lithium-ion module does not require nearly as much help from other sources due to its lower ESR and higher power density.

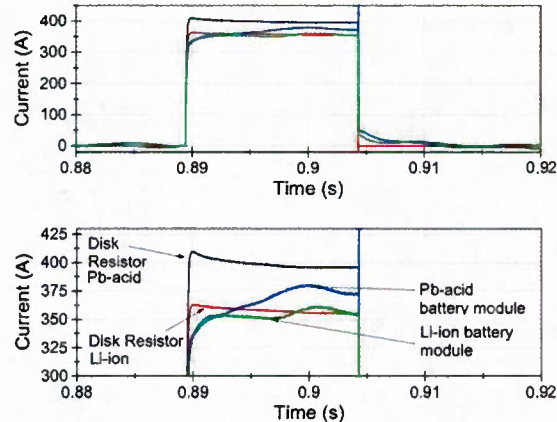


Figure 11. Current measured out of the battery modules and through the 50 mΩ high energy disk resistance. (lower graph is a zoomed in look at the peaks in the upper graph)

Finally, the voltage and current out of the inverter and across the 100 W light bulb for each energy storage type is shown in Figure 12. Other than the sharp transient at the end of the 15ms pulse, there is no noticeable impact to the inverter output. The transient is most likely noise induced on the diagnostics.

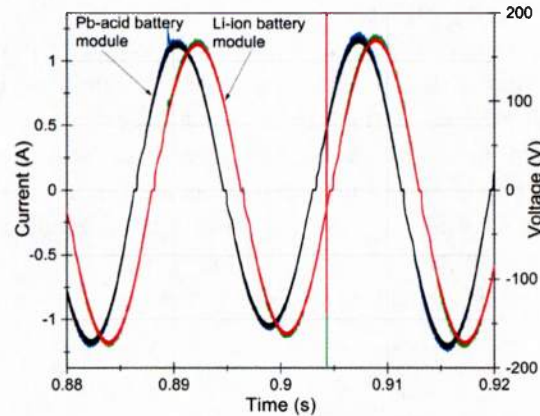


Figure 12. Voltage and current at the inverter output and to a standard 100 W light bulb.

These experiments give good insight into the capabilities developed at UTA using the funding from this grant. The results help lay a path forward for understanding the limitations of new high power electrochemical energy storage technologies for naval applications. These commissioning results show that a lithium-ion battery module does outperform a gel cell lead acid module when pulsed currents of ~400 A are drawn. It also opened our eyes to the impact the low impedance buffer capacitance installed on the various converters has when high pulsed loads are sourced.

AC Power Quality Experiments

In the second set of experiments presented here, the solar panels, wind turbines, and the PEM fuel cell have been left out of the grid to simplify the analysis, seen in Figure 13. Future phases of the research will integrate them. Prior to each experiment, the gasoline generator is operational and the prog. load is set to draw the desired constant power load at 120 VAC – 60 Hz. The DC/AC inverter is set to pass through the generator output to the prog. load and the DC charger are manually set on so that current is flowing into the batteries. The charger is capable of sourcing up to 55 A RMS in a 120 Hz pulsed fashion with duty cycle of 50%. After some time has passed, the IGBTs are closed connecting the DC bus to a 293 mΩ load resulting in roughly 80A of peak DC current flow. This setup was chosen to mimic the operation of a high DC pulsed load and high power AC load simultaneously. Eighteen experiments were performed with the prog. load set to draw 300 W initially, with that value being incremented by 100 W in each subsequent test. As the tests progressed, the pulsed load remained the same with the IGBTs connecting the load to the DC bus for 2 seconds.

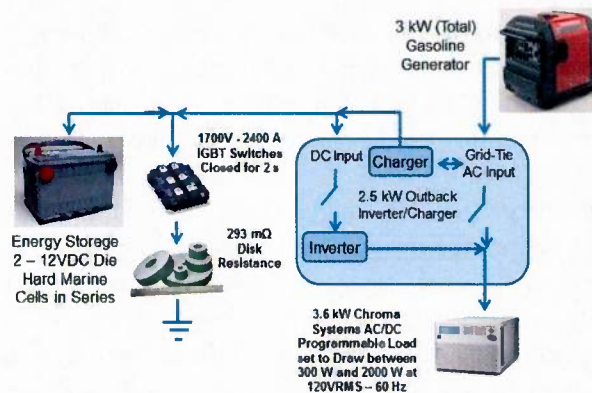


Figure 13. Section of the MicroGrid being used in the research presented here. (Note the Outback inverter schematic has been greatly simplified for presentation and is not representative of all the internal workings)

The performance of a MicroGrid was based on its ability to source quality power to connected loads within the standards set out by defined specifications, such as MIL-STD-1399-300B or IEEE-STD-519. In each of these standards, regulations are given which specify the allowable variance in the voltage, current, and frequency. The experiments performed here test the grid components to their extremes to evaluate how the various power quality metrics are affected. It should be mentioned that the components in our grids were not designed to meet these standards but they were good metrics anyway.

Three experiments will be highlighted here in which the prog. load is set at 300 W, 1300 W, and 2000 W respectively. The equivalent series impedance of the energy storage module is 4.2 mΩ while that of the charger is 3.2 mΩ. The voltage and current waveforms recorded from the energy storage during each of the three experiments are presented in Fig. 3, Fig. 4, and Fig. 5 respectively. The DC load is pulsed just shy of the 1s mark represented by the green trigger signal in the figures. The charger is supplying current to the batteries in a 120 Hz pulsed manner prior to the pulsed discharge. This is indicated by a positive current value. When the IGBT's are closed, the charger supplies current to both the energy storage and the resistive load since the charger's pulsed output voltage is higher than that of the energy storage. When the charger output voltage is low, the energy storage is solely responsible for supplying current to the pulsed load. Current sourced out of the batteries is represented by a negative current value. The batteries state of charge (SOC) decreases slowly as time increases.

During the experiment in which 300W is continuously drawn by the prog. load, the generator/charger is able to supply power to the prog. load as well as charge the batteries and source the 2.3 kW pulsed load.

As will be shown later, the quick transition from low power draw to a high power draw induces high fluctuations in the generator output frequency. By the end of the pulsed, the current sourced to the pulsed load decreases from roughly 81 A down to 79 A due to the slightly decreasing DC bus voltage. Keep in mind that 300 W is roughly 10% of the generator’s rated output power leaving the remaining 90% to source the pulsed load and batteries. As the batteries SOC, and therefore its terminal voltage, decreases the generator/charger are able to source higher current values in order to try and maintain a high rate of recharge. The increasing orange line drawn above the current waveform in Figure 14 is placed for presentation purposes only to highlight the rate of increased recharge current sourced to the batteries.

During the 1300 W experiment, it becomes harder for the generator/charger to source all three loads, those being the batteries, the pulsed load, and the prog. load. When the charger output is high, it is able to source the prog. load and the pulsed load but its voltage sags at a similar rate to that of the batteries limiting its recharge current as the battery voltage drops. The current supplied to the pulsed load by the charger decreases from 81 A down to 78 A in this experiment. This is highlighted again by the level orange line above the current waveform in Figure 15.

Finally when 2000 W is sourced to the prog. load, the generator and charger are unable to supply any recharge current to the batteries. The current supplied to the pulsed load by the charger decreases from 81 A down to 77 A in this experiment. The generator output voltage sags considerably with the batteries actually regulating the DC bus voltage when the pulsed load is sourced. This is shown in Figure 16 where the orange line actually decreases to zero quickly.

This data demonstrates the energy storage’s ability to back up high power transient loads when other sources begin to fall short. In future experiments, it is desirable to be able to control the operation of the charger in real time to enable the energy storage to take a more active role rather than restrict it to operation only when the charger output voltage is low.

As has been mentioned already, in all of the experiments the charger immediately increases its current output to the DC bus when the pulsed load is sourced. Plots of only the charger output current for the three tests above are shown Figure 17 – Figure 19 respectively.

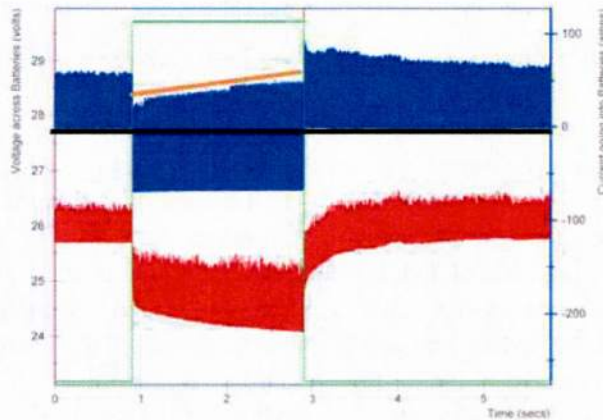


Figure 14. Energy storage voltage (red) and current (blue) during the 300 W AC prog. load test. Pulsed discharge time is highlighted by the green trigger pulse.

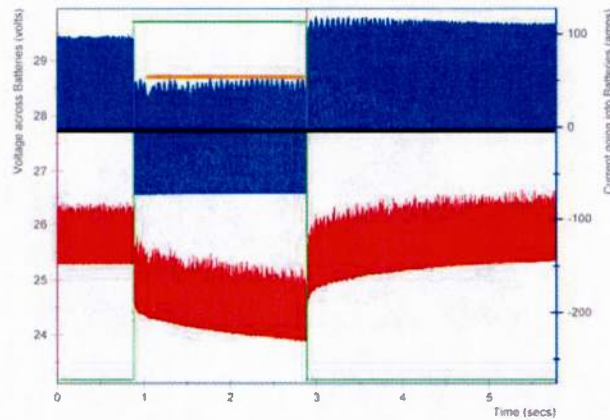


Figure 15. Energy storage voltage (red) and current (blue) during the 1300 W AC prog. load test.

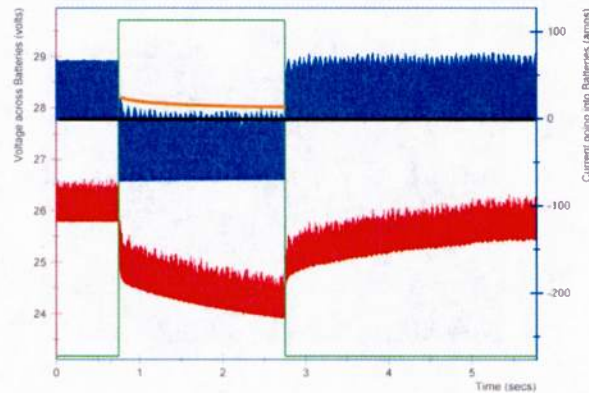


Figure 16. Energy storage voltage (red) and current (blue) during the 2000 W AC prog. load test.

In the 300 W experiment, the charger current output increases throughout the sourcing of the pulsed load as the voltage on the DC bus declines. During the 1300 W test, the maximum charging current is quickly sourced and it remains pretty constant throughout the pulse despite the decrease in the DC bus voltage. When the 2000 W experiment is performed, there is a quick spike in the output current followed by a very quick decline as the charger simply can't supply more power to the DC side of the system. This indicates that at the initial surge of current is more than likely supplied by the charger's output filter. Prior to the pulsed load, the charger maintained a steady charge current however after the pulsed load terminates, the current is unable to quickly return to the previous steady value. Supplying the AC load is the inverter's first priority while any remaining energy, which is decreased with each subsequent experiment, is able to supply power to the DC bus.

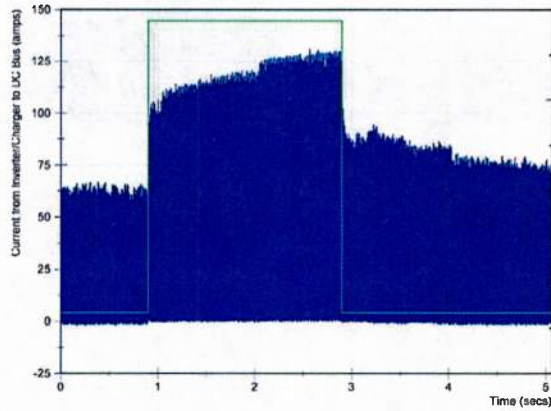


Figure 17. Charger output current during the 300 W experiment.

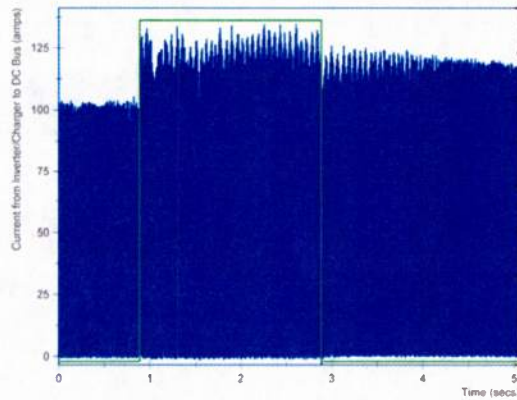


Figure 18. Charger output current during the 1300 W experiment.

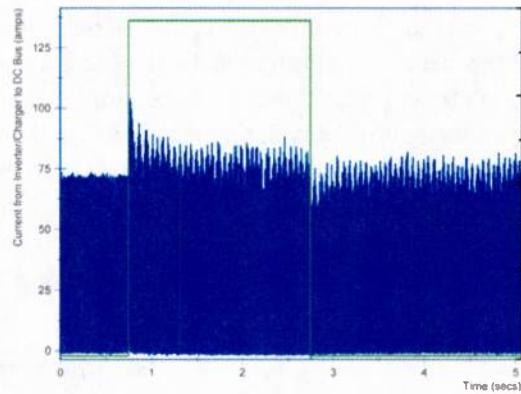


Figure 19. Charger output current during the 2000 W experiment.

The voltage recorded across the prog. AC load and generator, during the 300 W, 1300 W, and 2000 W experiments are presented in Figure 20 – Figure 22 and Figure 23 – Figure 25 respectively.

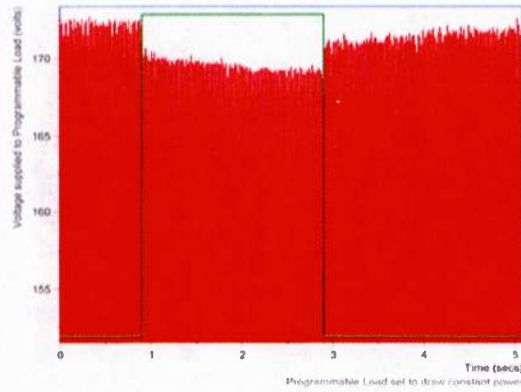


Figure 20. Prog. Load voltage during the 300 W experiment.

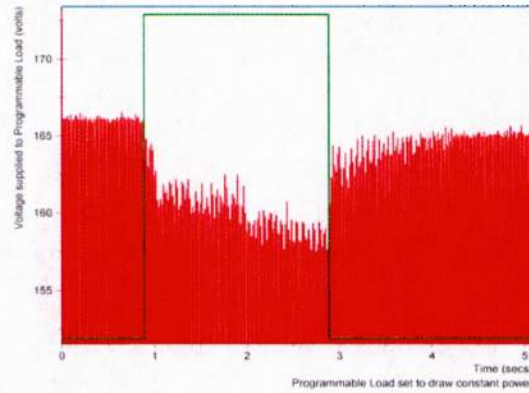


Figure 21. Prog. Load voltage during the 1300 W experiment.

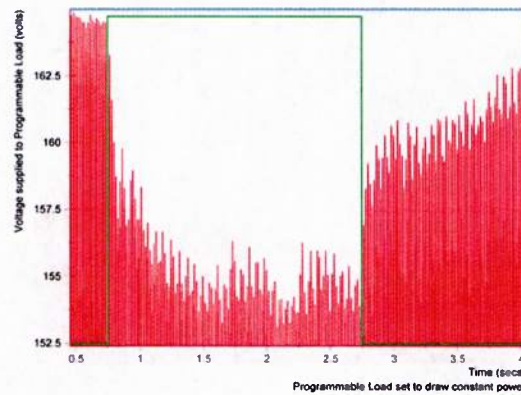


Figure 22. Prog. Load voltage during the 2000 W experiment.

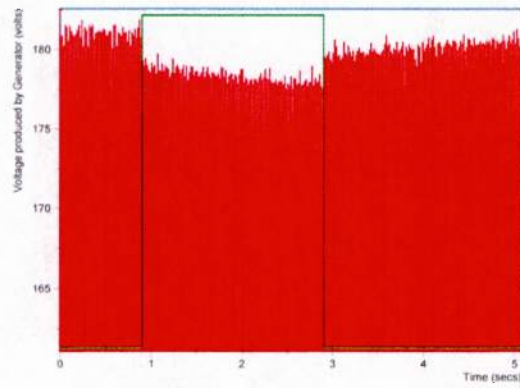


Figure 23. Generator voltage during the 300 W experiment.

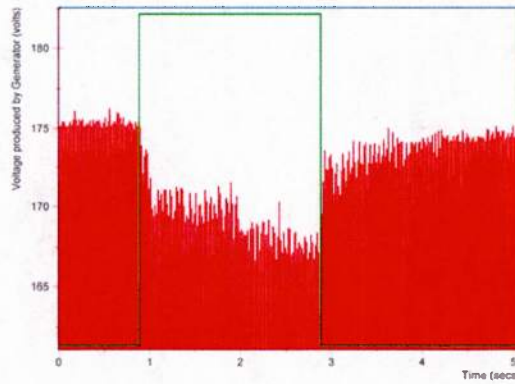


Figure 24. Generator voltage during the 1300 W experiment.

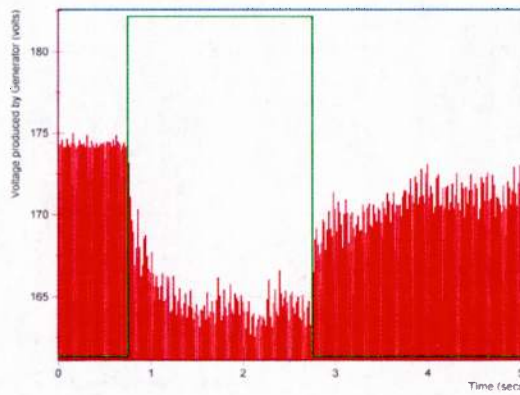


Figure 25. Generator voltage during the 2000 W experiment.

As expected, there are considerable sags in both of the AC voltages when the pulsed load is sourced. Sagging during and after the pulse occurs across all experiments and the severity increases as the AC load increases. Also as expected, the current drawn by the prog. load and sourced by the generator swells during the same time frame in order to maintain the constant AC load power. This is shown in Figure 26 – Figure 31 respectively.

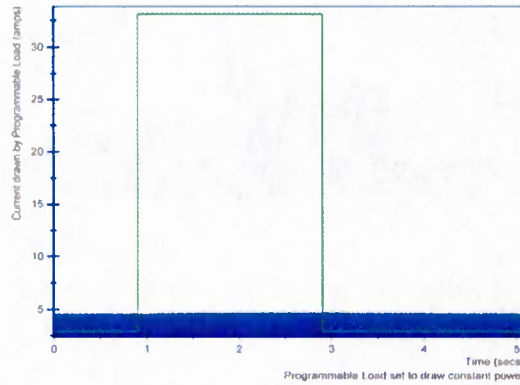


Figure 26. Prog. Load current during the 300 W experiment.

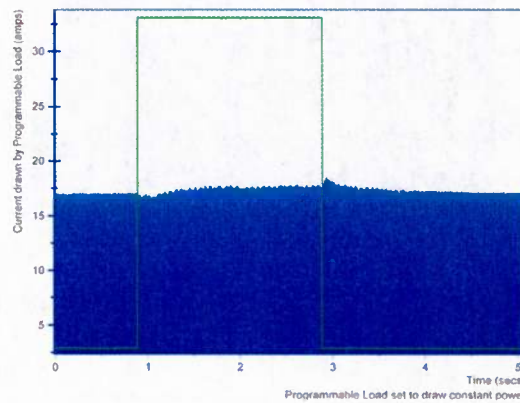


Figure 27. Prog. Load current during the 1300 W experiment.

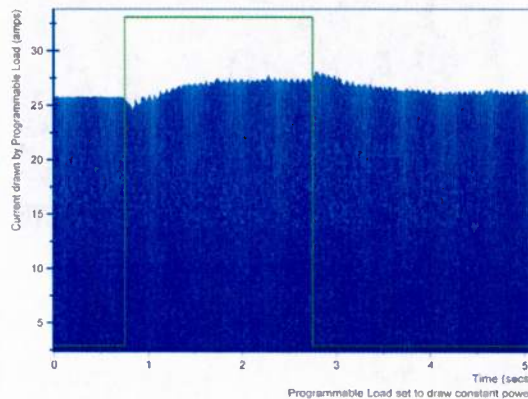


Figure 28. Prog. Load current during the 2000 W experiment.

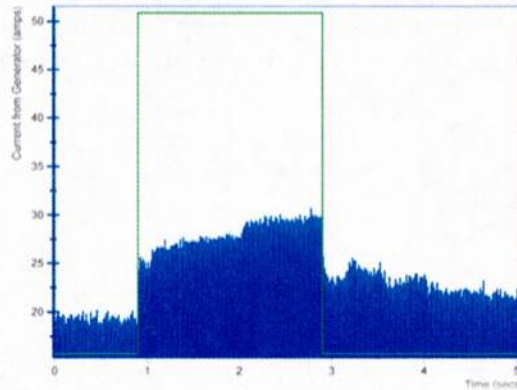


Figure 29. Generator current during the 300 W experiment.

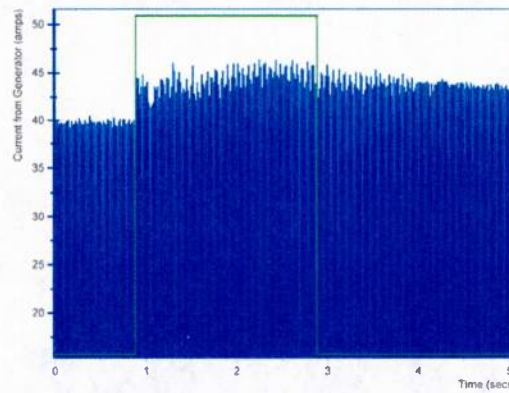


Figure 30. Generator current during the 1300 W experiment.

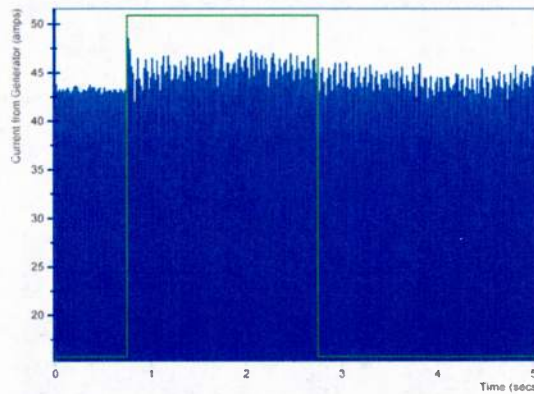


Figure 31. Generator current during the 2000 W experiment.

The current swells are most notable in the lower AC loading experiments. This is likely a result of the sudden transition from a low loading condition to a high loading condition when the pulsed load is triggered. The magnitude of the swell is limited of course by the maximum current the generator can

source. When the 1300 W load is sourced, the generator still has some available power to source. During the 2000 W experiment, the generator is already near its maximum. The pulsed load causes the current during and after the pulsed load to deviate much more compared to what it did before the pulsed load was sourced. Current deviation is not of consideration for most power quality analysis however, voltage deviation is and Figure 25 is reflective of generator voltage deviations.

In order to evaluate how the AC power quality is impacted due to these simultaneous loading conditions, the AC buses have been analyzed to see if they stay in accordance with the MIL-STD-1399-300B specification. The RMS values prior to the pulsed load and the minimum values recorded when the pulsed load is sourced are listed in Table I.

TABLE I. GENERATOR AND AC LOAD RMS VOLTAGES

<i>Voltage (RMS)</i>	<i>300 W Exp.</i>	<i>1300 W Exp</i>	<i>2000 W Exp.</i>
Generator Max.	128.24 V	123.95 V	123.32 V
Generator Min.	125.65 V	118.19 V	115.42 V
AC Load Max.	121.90 V	117.43 V	116.30 V
AC Load Min.	119.50 V	111.53 V	109.21 V

The frequency tolerance listed in MIL-STD-1399-300B for a single phase, 120 VAC - 60 Hz power system is between 58.2 Hz and 61.8 Hz. The acceptable continuous voltage range is listed between 109 VAC and 121 VAC. For short durations up to 2 seconds, the allowable range is between 92 VAC and 138 VAC. In all of the experiments presented here, the AC bus voltages stayed well within the continuous bounds. During the 2000 W experiment, the continuous voltage range condition was nearly violated. The allowed AC voltage amplitude modulation is 2% and the allowable AC frequency modulation is 0.5%. The allowed total harmonic distortion (THD) is 5% and the ratio in percent of the greatest amplitude of a single harmonic over the fundamental frequency is 3% [9]. In comparison the standards listed in the IEEE-STD-519, which were developed for use in large scale electric power systems, have the same tolerances for the THD, highest single harmonic and frequency modulation, and a tighter tolerance of 0.5% on the voltage amplitude modulation [10]. Tables II and III present the results obtained from the frequency and modulation analysis of the two AC buses in the system. The analysis was performed using the techniques highlighted in the MIL-STD-1399-300B.

TABLE II. GENERATOR POWER QUALITY ANALYSIS

<i>Generator</i>	<i>300 W</i>	<i>1300</i>	<i>2000</i>
Amp. Modulation	1.11%	2.71%	3.68%
Freq. Modulation	0.60%	0.15%	0.24%
Highest Harmonic	0.70%	0.67%	0.59%
THD	1.08%	1.24%	0.89%

TABLE III. PROG. AC LOAD POWER QUALITY ANALYSIS

<i>AC Load (Voltage)</i>	<i>300 W</i>	<i>1300</i>	<i>2000</i>
Amp. Modulation	1.21%	2.74%	3.72%
Freq. Modulation	0.85%	0.75%	0.78%
Highest Harmonic	0.76%	0.44%	0.52%
THD	1.02%	0.66%	1.02%

The generator’s open circuit fundamental frequency is 59.9 Hz. The THD and the value of the highest harmonic, the third harmonic, all fall within the bounds set by the MIL-STD-1399, but are out of the bounds set by IEEE-STD-519. The voltage amplitude and frequency modulation values fall out of bounds for the AC load in nearly all of the experiments performed, however the generator is only out of

frequency specification during the light load experiment and out of voltage specification during the higher load experiments. This shows that the inverters pass thru is a direct connection between its AC input and AC output buses. The generator shows increased frequency stability with increased loading and as expected the voltage modulation falls as the load increases. None of the RMS voltages measured fell out of the specified voltage range given in Figure 13 of MIL-STD-1399-300B [9]. The generator's best power quality was observed when the initial loading was high. The AC load's power quality was best when medium power levels were sourced.

Conclusion

These results obtained from the work supported through this grant show that there are many configuration and operational concerns that need to be addressed in order to simultaneously source high pulsed and continuous loads in a MicroGrid architecture. Accurate control and monitoring is needed to ensure that operational electrical standards are always maintained and critical loads are sourced. MicroGrids are very promising electrical grid architectures for use on both land based and moveable platforms. Future work is planned at UTA to continue to flush out the answers to these concerns so that the DoD can make these platforms a future reality. Additional regulation of the energy storage will be installed so that hybrid energy storage configurations which optimize the installation of energy dense and power dense technologies can be developed and evaluated. A more accurate control of the inverter/charger will also be implemented in order to better regulate its operation.

References

- [1] Schulz, N.N.; Hebner, R.E.; Dale, S.; Dougal, R.; Sudhoff, S.; Zivi, E.; Chrysostomidis, C.; , "The U.S. ESRDC advances power system research for shipboard systems," Universities Power Engineering Conference, 2008. UPEC 2008. 43rd International , vol., no., pp.1-4, 1-4 Sept. 2008.
- [2] Franklin H. Holcomb. Hybrid-Intelligent POWER "HI-POWER", 2008 High-Megawatt Power Converter Technology R&D Roadmap Workshop, NIST, Gaithersburg, MD, April 8, 2008.
- [3] R. E. Hebner, "Energy Storage in Future Electrical Ships," Electric Ship Research and Development Consortium, Tech. Rep. [Online] <http://www.esrdc.com/docfiles/energystorageinfutureelectricshipsmarch2008.pdf>.
- [4] Next Generation Integrated Power System, NGIPS Technology Development Roadmap, Ser 05D / 349, November 30, 2007.
- [5] Office of Naval Research. "Hybrid Energy Storage Module (HESM): Ammednment 001" 13-SN-0007 [Online]. Available: <http://www.onr.navy.mil/~media/Files/Funding-Announcements/Special-Notice/2013/13-SN-0007-Amendment-0001.ashx>. [Accessed 20 Jan 2013]
- [6] L.V.L Abreu and M. Shahidehpour, 'Wind Energy and Power System Inertia,' IEEE Power Engineering Society General Meeting, 2006.
- [7] Data sheets for the GAIA 27 Ah Lithium-ion cell, http://www.gaia-akku.com/fileadmin/user_upload/downloads/cells/27AhHP_NCA.pdf, October 28, 2011.
- [8] Diehard Products Marine and RV, <http://www.diehard.com/products/marine-and-rv>, KCD IP, LLC., April 13, 2012
- [9] Department of Defense Interface Standard Section 300B, MIL-STD-1399, 1992.

- [10] IEEE Recommended Practices and Requirements for Harmonic Control in Electrical Power Systems, IEEE Standard 519, 1992.

Papers Authored and Presentations Given

- [1] **D.A. Wetz**, B. Shrestha, P. Novak, and Y. Chen, ‘Characterization of High Power Electrochemical Energy Storage Devices for use in Naval Applications,’ Proceedings of the American Society of Naval Engineers Electric Machines Technology Symposium (EMTS) 2012, Philadelphia, Pennsylvania, May 23-24, 2012. (Oral Presentation)
- [2] **D.A. Wetz**, B. Shrestha, P. Novak, and Y. Chen, ‘Characterization of High Power Electrochemical Energy Storage Devices for use in Naval Applications,’ *Accepted for publication in the September 2013 issue of the ASNE Journal, Publication Pending.*
- [3] J.P. Kelley, **D.A. Wetz**, J.A. Reed, I.J. Cohen, G. K. Turner, and W.-J. Lee, ‘The Impact of Power Quality when High Power Pulsed DC and Continuous AC Loads are Simultaneously Operated on a MicroGrid Testbed,’ Manuscript submitted to the IEEE Electric Ship Technologies Symposium 2013, April 22 – 24, 2012, Arlington, Virginia. (Oral Presentation)

Students Supported

1. Jay Paul Kelley (Masters Student in Electrical Engineering)

Acknowledgments

The authors wish to express sincere gratitude to both the US Office of Naval Research (ONR) and the US Department of Energy (DoE) for their respective financial supports which helped to make this work possible. Any opinions, findings, and conclusions or recommendations expressed in this publication are those of the authors and do not necessarily reflect the views of the US ONR or US DoE.